SOFT ROBOTICS
Volume 3, Number 3, 2016

DOI: 10.1089/soro.2016.0027

SoRo
Soft Robotics

ORIGINAL ARTICLE

A Novel, Variable Stiffness Robotic Gripper Based on Integrated Soft Actuating and Particle Jamming

Ying Wei, Yonghua Chen, Tao Ren, Qiao Chen, Changxin Yan, Yang Yang, and Yingtian Li

Abstract

This article presents the design principle and fabrication of a variable stiffness soft robotic gripper for adaptive grasping and robust holding. The proposed robotic gripper is based on a finger design that combines a fiber-reinforced soft actuator and a particle pack. The soft actuator is responsible for the bending motion of the finger, and the particle pack acts as a stiffness-changeable interface between the finger and the object. In the natural state, the particle pack is soft and adaptive to part geometry. It can rapidly stiffen (through vacuum) to resist external load or to freeze the currently bent contour of the finger. Experimental studies have shown that more than a 10-fold stiffness enhancement is achievable. Therefore, the proposed gripper is capable of handling objects with different shapes, weights, and rigidities, which have been a great challenge for robotic grasping. For more effective grasping, a grasping strategy is designed for the proposed soft gripper with simultaneous consideration of grasping adaption and robustness.

Keywords: variable stiffness, soft gripper, adaptive gripper, particle jamming, soft robot

Introduction

Human hands can grasp objects of various shapes regardless of whether they are fragile or highly deformable,[1] which provide a promising model for robotic grasping researches. To mimic the dexterity and versatility of human grasps, traditional robotic grippers have to rely on complex sensing, predefined kinematics, delicate modeling, and control system.[2–4] They are generally used in well-defined environments for specific tasks. As a result, conventional rigid body-based manipulators with the versatility of dexterous grasping are costly, slow, application specific, and difficult to develop.

Soft actuators[5–7] made of entirely soft material, often elastomeric material, provide a promising path to biomimic gripper design due to their remarkable capability of handling fragile objects and adapting to unknown and irregular shapes. The utilization of soft material in robotics brings about much safer interaction with surroundings and humans when dealing with various tasks in grasping in an uncertain environment. Soft actuators can be actuated by a variety of methods: compressed fluids,[6,8,9] chemical reaction,[10] tendon,[11,12] shape memory effect (e.g., shape memory alloy),[13,14] and electrical charges.[15,16] Researchers have developed several soft manipulators based on pneumatic networks.[8] These manipulators have shown remarkable flexibility and dexterity, in that they can handle fragile objects such as eggs and flowers with very simple control. However, the inherent weakness of low stiffness limits the applications of such soft manipulators. Soft grippers actuated by cable tension are developed for minimally invasive surgery.[11] The gripper shows good performance, but the cable-driven method requires that the robot body must be strong enough to endure tension force, which is impractical for soft robots. A novel type of soft gripper based on electrostatic actuation with intrinsic electroadhesion force[17] can manipulate deformable fragile objects of any shape with a single control signal. Yet, the high driving voltage contradicts our expectations about soft robots being safe and environment friendly. Safety in human–machine interaction is a main consideration for robotic grasping. Hence, in this design, pneumatic power has been used for the proposed gripper. Its property of compressibility decides that it has the congenital advantage of compliance and safe contact with surroundings.

The soft property also brings about a challenge for air-driven soft robot to support load and to maintain its position under external stimulus. For a soft robot hand, it is desirable to freely move and adapt to surroundings or shape contours at low stiffness and to stiffen to apply force when needed in object manipulation. Variable stiffness is a promising solution to make up the weakness of pneumatic soft robots.

Department of Mechanical Engineering, The University of Hong Kong, Hong Kong, China.

In fact, the human hand is a great example, whose variable stiffness results from muscle's ability of transition between passive state (low stiffness) and active state (high stiffness). Our hands are extremely flexible and compliant (low stiffness) in natural state or when we feel and touch an object with great care. We can easily handle fragile objects, even those highly deformable ones. Meanwhile, we are capable of grasping and retaining heavy objects when the hand muscle stiffens. The large range of variable stiffness is crucial for the human hand to be universal and to be reliable. For the same reason, the application of variable stiffness into the soft robotic gripper can greatly improve its grasping performance.

Several materials and methods have been applied to soft robots to realize variable stiffness such as heat-sensitive function material,[18,19] magnetorheological (MR) or Electrorheological (ER) fluid,[20,21] particle jamming,[22–25] dielectric elastomers (DEAs),[26] and cable tension-based system. All these methods show prominent performance of variable stiffness. However, heat-sensitive function materials such as shape memory alloys require relatively long heating time to activate and the cable tension method suffers the same problems as they are applied as actuators. MR and ER fluids require external fields and high driving voltage, which is unsafe for interaction with humans. DEAs require high voltage, which is undesirable for many applications. In contrast, particle jamming has the advantages of simple mechanism, quick response, large range of stiffness variation, and easy controllability: particles are loosely packed within an enclosed membrane that can conform to contact surface with compliance and flexibility. When the pressure is reduced by a vacuum pump, particles are jammed together firmly and exhibit high stiffness. Therefore, particle jamming is a more desirable option for soft grasping. In addition, both pneumatic actuator and jamming can be activated by air pressure, leading to system simplicity.

In this article, we demonstrate a novel design of a compliant robotic gripper based on pneumatic soft actuator and particle jamming. The proposed multifingered gripper can passively conform to object geometries and execute robust grasping. Figure 1a shows the basic design concept of the proposed soft finger. It is constructed based on the combination of a fiber-reinforced soft actuator and a particle chamber enclosed by an elastomeric membrane. The flexible, but inextensible, fibers arranged along the length of the soft actuator can simplify the manufacturing process[9] because the inner pneumatic channel is a straight-through channel as tubular geometry rather than individual segments with different geometry. The elastomeric elements augmented by fibers deform more equally with limited stress during pneumatic actuation and the actuator can output large force. The actuator generates a bending motion when inflated, as shown in Figure 1b. The modulation of the finger stiffness is realized by the particle-jamming principle. In the natural state, the particles are loosely enclosed in the membrane chamber to form a soft and flexible structure, as shown in Figure 1a. Particles inside the membrane will pack firmly under vacuum pressure, thus the tube will stiffen consequently. There is a big difference between the maximum weights lifted by the finger with and without particle jamming (Fig. 1b). Theoretically, a wide range of actuator stiffness can be achieved by modulating vacuum pressure.

Researchers have been developing soft grippers based on particle jamming. A universal particle-jamming gripper has been reported.[22,27] The basic design is shown in Figure 2a. It is a ball-type membrane filled with coffee grains. The gripper can grasp objects of very different shapes, weights, and fragility, while its ball shape makes it difficult to grasp objects with no sharp edges such as an apple in Figure 2b or objects with soft body as in Figure 2c. The requirement on preloading force along normal or sheer direction weakens its universality and limits its grasping postures. In Figure 2d, for instance, the gripper can easily grasp a coffee mug from the desk in a downward bevel direction, but cannot make it in a horizontal approaching orientation if the desk surface is very smooth. As a comparison, a finger-based hand shown in Figure 2e is more dexterous.

The soft gripper proposed in this article has the advantages of both particle jamming and soft actuation. In the natural state, the gripper is highly compliant and can adapt to the object shape, which greatly enhances the grasping reliability. After grasping an object, the gripper is stiffened by particle jamming to freeze its current position so that it has the strength to move the object and resist external disturbances. Therefore, the novel gripper design allows a much fuller contact with the object, which has been a challenge for existing grippers.

The Proposed Gripper Design

Since the source that nature uses to build human hands is far superior to that brought by modern technologies, the types of robotic hands are mainly decided by what we expect from them.[28] For current works on soft robotic hands, the performance of a dexterous grasp and the capability of firm holding are always treated independently since they inherently contradict each other for soft robotic hands. However, it seems that human grasp has rarely encountered such a problem. The reason can be attributed to the inability of current soft robotic hands to vary stiffness within a large range. The integration of soft actuator with particle jamming allows the proposed robotic hand to have a large stiffness variation range potentially.

The gripper configuration

Human fingers have four basic kinds of motion: flexion, extension, adduction, and abduction. These motions allow

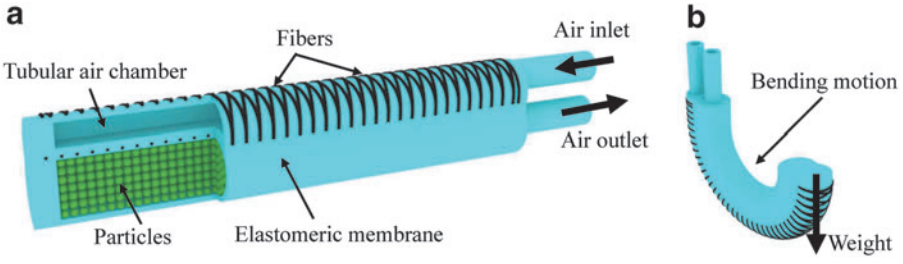

FIG. 1. Concept of the proposed soft robotic finger. **(a)** Design features. **(b)** Expected bending motion. Color images available online at www.liebertpub.com/soro

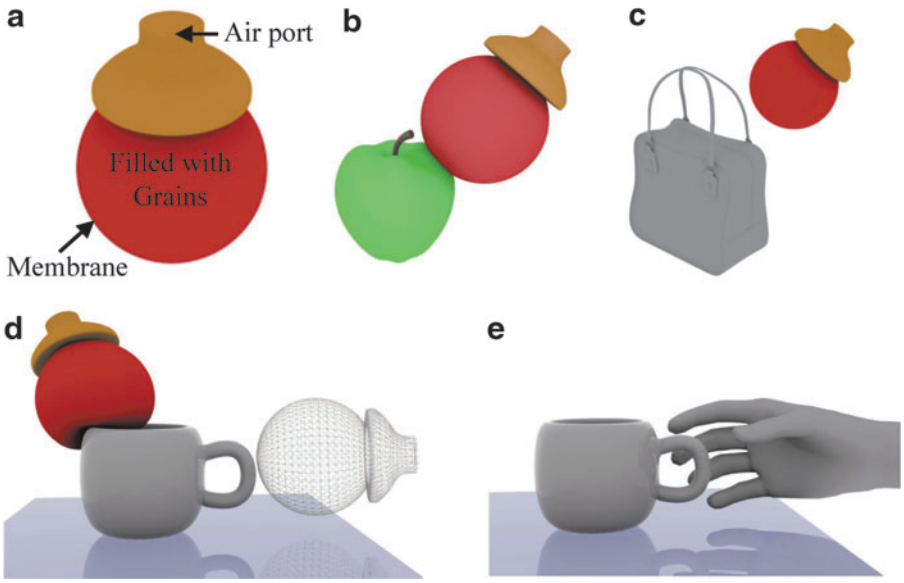

FIG. 2. Comparison of ball-type jamming gripper and multifingered gripper. **(a)** Ball-type jamming gripper design,[22,27] **(b)** object with no sharp edges, **(c)** soft object, and **(d)** limited grasping postures. **(e)** More versatile finger-based gripper. Color images available online at www.liebertpub.com/soro

the fingers to bend toward the palm or contrariwise and to adduct to the middle finger or abduct. The thumb has the fifth motion that it can approach all the other fingers to realize a set of whole grasps with a changing rotation axis.[29] The imitation of anthropomorphic motion is very difficult for soft actuators. Hence, in our prototype gripper design, all fingers are the same and configured as shown in Figure 3a.

The placement of fingers will determine the size of objects that can be grasped and manipulated. As shown in Figure 3b, the fingers are installed parallel, and the size of an object that can be grasped is limited by the length L. Therefore, it is desirable to configure fingers as in Figure 3c with a specific angle θ to the gripper base. To ensure reliable grasping, the finger tips should have space to deform. Figure 3c shows the smallest and largest ball sizes that the gripper can reliably grasp. Suppose the fingers have an assembly angle θ, an assembly distance l, and a finger length m, the hand can manipulate objects with the size from R_{min} to R_{max} in radius. According to Figure 3c, the minimum ball size R_{min} is as follows:

$$R_{\min} = r = \frac{l}{2}\tan\theta \tag{1}$$

The largest value of R is limited by the maximum distance, L, between two finger tips. Figure 3d shows the maximum size of object with R in radius that the hand can manipulate. Suppose the object weight is G, equating forces in the vertical direction we have the following:

$$G + 2F\sin\varphi = 2F\mu\cos\varphi \tag{2}$$

where $\varphi = \pi/2 - \theta$.

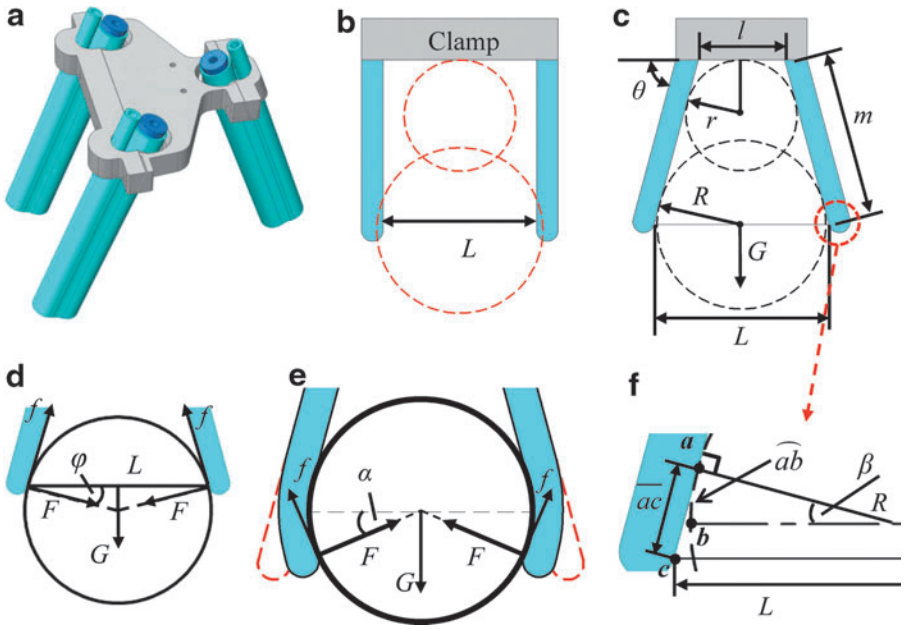

FIG. 3. Gripper configuration. **(a)** Diagram of proposed gripper. **(b)** Limitation when the fingers are *parallel*. **(c)** Larger gripping volume. **(d)** Forces when no wrapping, **(e)** forces with wrapping, and **(f)** magnified force diagram. Color images available online at www.liebertpub.com/soro

Then,

$$\Rightarrow \begin{array}{l} G = 2F(\mu \sin\theta - \cos\theta) \\ F = G/2(\mu \sin\theta - \cos\theta) \end{array} \quad (3)$$

According to Equation (3), the grasp ability is related to grasping force, F, provided by the actuator and the friction coefficient μ. The output force of a soft actuator is inherently small due to its soft material nature and the actuation method. Therefore, the grasping ability is directly decided by the friction between the fingers and the objects, and the friction coefficient μ must be larger than $\cos(\theta)$. It is not stable and reliable because friction is highly sensitive to surface texture and contact surface area, and slight unevenness or contamination on the contact surface may cause failure in grasp. On the contrary, if the deformed finger under compressed air can wrap around more than half of the object as shown in Figure 3e, the case will be different as

$$\Rightarrow \begin{array}{l} G = 2F(\mu \sin\alpha + \cos\alpha) \\ F = G/2(\mu \sin\alpha + \cos\alpha) \end{array} \quad (4)$$

In this case, the hand performs much more reliable grasping compared with Equation (3) and the hand is able to grasp even if μ is smaller than $\cos(\theta)$ according to Equation (5). The larger the area the deformed finger can cover, the heavier the weight the hand can handle. To guarantee that the deformed finger wraps around more than half of the object, $\overline{ab}$ should be longer than $\widehat{ab}$ shown as Figure 3f:

$$m - \left(R\sin\theta - \frac{l}{2}\right) \Big/ \cos\theta > \beta R \quad (5)$$

where $\beta = \pi/2 - \theta$.

Therefore,

$$R_{\max} < \left(m + l/2\cos\theta\right) \Big/ \left(\frac{\pi}{2} - \theta + \tan\theta\right) \quad (6)$$

and the value of α in Equation (5):

$$\begin{array}{l} \alpha = (\overline{ac} - \widehat{ab})/R \\ \Rightarrow \alpha = \dfrac{m}{R} + \dfrac{l}{2R\cos\theta} + \theta - \dfrac{\pi}{2} - \tan\theta \end{array} \quad (7)$$

For the design with specific values of m, l, and θ, the robotic hand can manipulate an object ranging from R_{min} to R_{max} with grasping capability calculated using Equations (5) and (7).

Compliance and passive adaption

The capability of exploiting the compliance of tissue in the finger is a significant reason to explain why the human hand can easily pick up objects with a variety of shapes. The compliance of a robotic gripper and its adaption to objects' contour can also guarantee safe and reliable contact between the gripper and the target object, which is essential for reliable grasping and holding. Most current robotic grippers tend to function well to a specific set of objects with relatively regular shape or contour, such as a cylinder, sphere, and cuboid. There is always a problem when the object shape is irregular. In the real world, most objects present uneven surfaces, irregular shapes, and complex contour. It is a great challenge for robotic grippers to adapt to objects' surface shapes. Although soft robots have great compliance and safe interaction with objects and the surroundings, they cannot adapt to smaller features as shown in Figure 4a. In Figure 4a, a large free space exists between the soft fingers and the object, which may cause failure during grasp and handling. When an object is grasped along the horizontal direction, its uneven surface is likely to cause trouble as well. The grasp state is easy to break down and to fail if the fingers happen to have contact with the largest margin of the object shown as the solid line in Figure 4b, while the contact situation represented by the red dashed line results in a twist on actuator, which affects its stiffness.

However, the adaption problem can be effectively solved by our design. In the natural state, the mechanism has the inherent advantage of passive adaption and compliance with contact surface since particles can freely flow inside the membrane. The uneven surface and irregular contour of an object inversely promote a better contact with the fingers, as shown in Figure 4c–e. Whatever the grasping direction is, horizontal or vertical, even for the irregular shape like Figure 4e, the grasping contact can adapt well using our soft gripper. The passive adaption driven by active actuation leads to closer contact between the fingers and the object, and this provides fundamental advantages for stable and reliable grasping. When object manipulation is required, vacuum

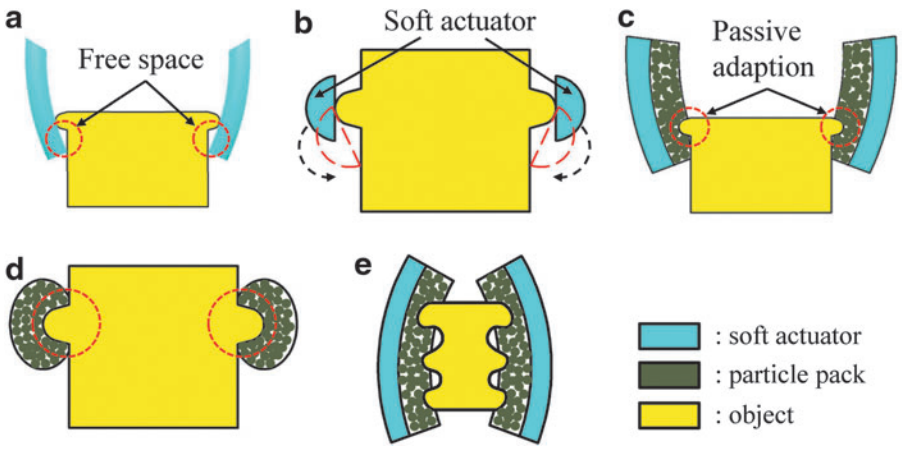

FIG. 4. Diagram of compliance and passive adaption. **(a)** Vertical grasping of soft grippers. **(b)** Horizontal grasping of soft grippers. **(c)** Vertical grasping of the proposed gripper, **(d)** horizontal grasping of the proposed gripper, and **(e)** reliable grasping of irregular shape objects. Color images available online at www.liebertpub.com/soro

pressure can be activated and the particles stiffened to increase rigidity of grasping.

Prototype Fabrication

The prototype robotic gripper consists of three highly compliant and stiffness-changeable soft fingers. A finger has two parts: the actuation part and the stiffening part. The actuation part adopts flexible fiber-reinforced soft actuator, inspired by related works.[9,30–32] The soft actuator is fabricated with three different materials as shown Figure 5a–d: elastomeric rubber, an inextensible but flexible plate, and fibers. The inextensible plate works as the passive layer, which disables the elongation of the actuator bottom layer, while the other soft body acts as an active layer. Under compressed air, the different elongation between the active layer and the passive layer causes bending motion of the whole actuator body. Circumferential reinforcement provided by wrapped fibers limits expansion along the radial direction and promotes linear elongation, hence greater bending performance. Besides, the elastomeric elements augmented by fibers deform more equally with limited stress during pneumatic actuation, thus the actuator can withstand higher pressure and output larger force. The stiffening part is a simple cylinder made of silicone rubber and filled with small particles, as depicted in Figure 5e–g. This part can be stiffened by vacuum pressure. The cylindrical geometry allows for better contact with objects of various geometries, which suggests better grasp performance.

Fabrication of the fingers is accomplished quickly with the aid of additive manufacturing (AM) technologies. AM technologies, also known as 3D printing, provide a convenient way to fabricate an object layer by layer, as opposed to conventional methods. In this research, we use an AM machine Objet Eden350V for mold making. FullCure 705, a nontoxic gel-like photopolymer, is used as the support material and VeroClear 950 as the mold material. The print resolution is 42 μ along X and Y axes, and 16 μ along the Z axis. The 3D printing of all molds takes about 8 h. The multistep molding process of an individual finger is illustrated in Figure 5:

(1) Casting the first rubber layer by using a closed two-part mold and an inner core, as shown in Figure 5a. To ensure repeatability, all molds are 3D printed with high resolution (0.042 mm). The end of the molded first layer is uncapped with a hemicircle elastomeric air chamber.
(2) Attaching the inextensible but flexible plate to the bottom of the first layer and winding fibers along the groove features on the exterior surface, as shown in Figure 5b.
(3) Recasting the fiber-reinforced part in another thin layer of silicone to fix the fibers and the plate, as in Figure 5c.

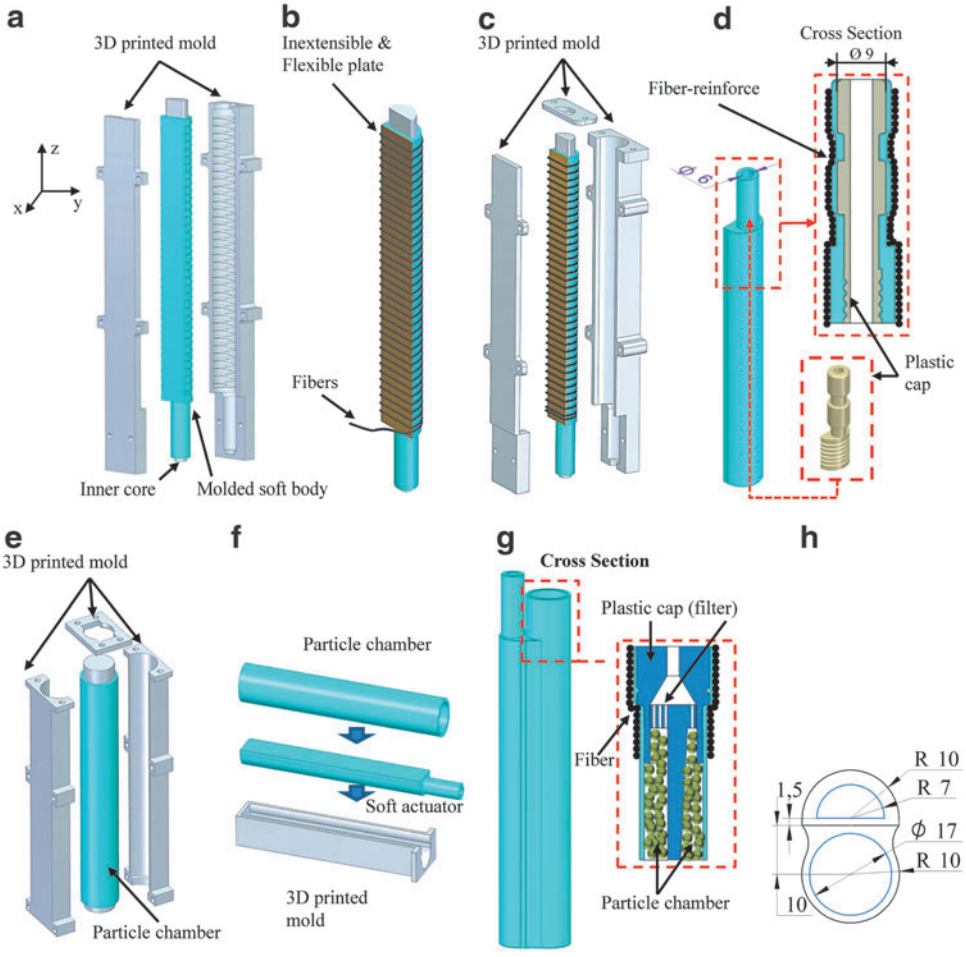

FIG. 5. Manufacturing process of a soft finger. **(a)** Molding the first layer. **(b)** Attaching inextensible plate and reinforcing by fibers. **(c)** Recasting. **(d)** Sealing. **(e)** Molding the membrane of particle sac. **(f)** Assembly. **(g)** Filling particles and capping. **(h)** Size details of cross section. Color images available online at www.liebertpub.com/soro

(4) Inserting the 3D printed rigid cap through the bottom end. Inspired by conventional sealing method using sealing washer and O-ring, the size of the upper part's cap is designed to be a little larger than that of the soft body marked by a red line in Figure 5d. Reinforced by fibers with pasty silicone adhesive, it shows great sealing performance.
(5) Casting a particle chamber with 3D printed molds, as shown in Figure 5e. The chamber is designed in simple cylindrical geometry to gain isotropic property and compliant contact with objects.
(6) Assembling the particle chamber and soft actuator together by silicone.
(7) Capping the bottom end of the integrated actuator first and then filling the cylindrical particle chamber with small particles. The stiffening chamber also needs good sealing because it must retain vacuum pressure to gain stiffness. A printed rigid cap with filter function is inserted into the chamber, as shown in Figure 5g. Reinforced by fibers with pasty silicone adhesive, the simple method provides great sealing performance.

The shape and size of actuator are detailed in Figure 5e. According to the analysis in Section 2.1 on gripper configuration, the proposed robotic gripper can manipulate object sizes in the range 65–142 mm when relevant gripper dimensions in Figure 3 are set as $l = 50$ mm, $m = 135$ mm, and $\theta = 70^{\circ}$.

Experiment and Analysis

In this section, we test the finger's performance on stiffness variation. It is common knowledge that our hand becomes very rigid when all the fingers flex toward the palm, while it is soft and compliant when all fingers are stretched outward. This is enabled by the variable stiffness of muscles around finger joints. This feature allows us to deal with fragile lightweight objects as well as heavier objects. The low stiffness can reduce force peak and abnormal impulse occurred at the contact area between the object and the hand to ensure safe interaction. It is also desirable for a robot to freely move and adapt to different environments at low stiffness and to increase stiffness to apply force or manipulate an object when needed, just like human muscles.

Stiffness experiment

Stiffness represents an object's capability of resisting deformation in response to external forces.[33] In this research, we describe stiffness by using a force F that results in a displacement X, as shown in Figure 6. Considering the unidirectional actuation nature of the proposed soft finger, loading can be classified into two loading conditions: (1) external force F_1 with corresponding displacement X_1 along the bending plane (axial) as shown in Figure 6a and (2) the force F_2 with corresponding displacement X_2 perpendicular to the axial plane as shown in Figure 6b. The actual laboratory setup is shown in Figure 6c. For each loading condition, we will have two sets of data, one with vacuum pressure and the other without.

In the test setup as shown in Figure 6a, the finger is actuated by an air pressure of 0.08 MPa. A pulling cord connects the tip of the testing finger with a force sensor through two pulleys. The friction force introduced by the pulleys is so small that it can be neglected. The resolution of the force sensor is 0.01N. The pulling cord needs to be pretensioned with 0.05N before each test and the length L is measured at 84 mm in this experiment. During measurement, the force sensor is pulled away from the finger along a linear guide. A vacuum pump is used to provide vacuum. Its pressure is controlled within the range of 0 KPa to −90 KPa. Particle jamming is disabled when the pump does not function or when the vacuum pressure is 0 KPa. The particle pack can be rapidly stiffened when vacuum pressure is switched to −90 KPa. The rigidity of the finger under different vacuum pressures is measured and the results are plotted. Figure 7a shows the relationship of F_1 versus X_1 when force direction is along the axial bending plane as in Figure 6a, and Figure 7b demonstrates the variation of F_2 with respect to X_2 when force direction is in the transverse bending plane as in Figure 6b.

According to the definition of stiffness, the slope of the curve in Figure 7a, b represents the stiffness level of the finger. The greater the slope is, the higher the stiffness of the finger. It is clearly shown in Figure 7a, b that regardless of the force direction, the finger stiffness is much smaller without vacuum pressure compared with finger stiffness with vacuum pressure at −90KPa for particle jamming. Therefore,

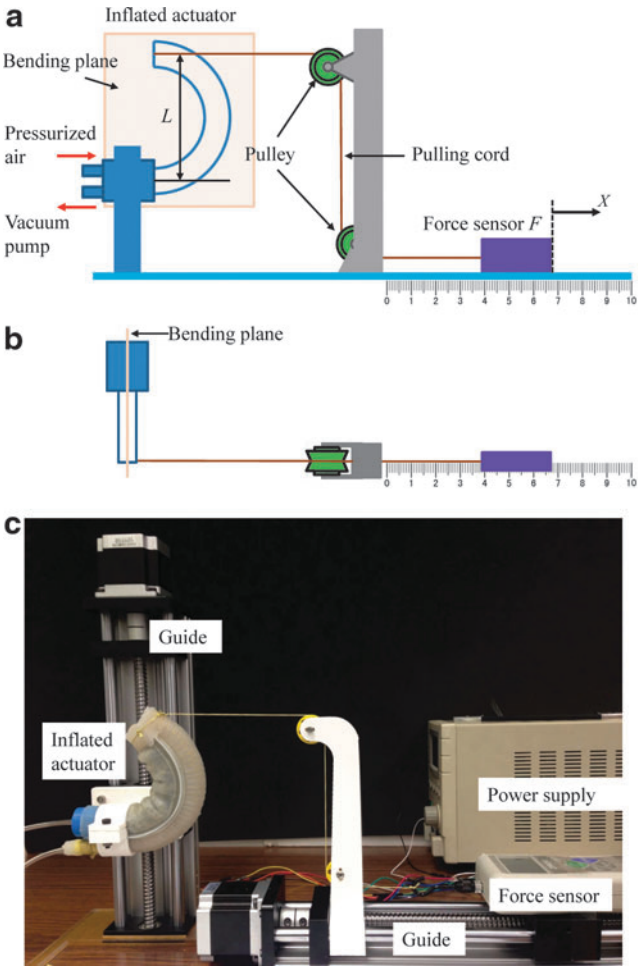

FIG. 6. Test setup. **(a)** Measurement for lateral *bending plane*. **(b)** Measurement for transverse *bending plane*. **(c)** The actual setup for the lateral *bending plane* measurement. Color images available online at www.liebertpub.com/soro

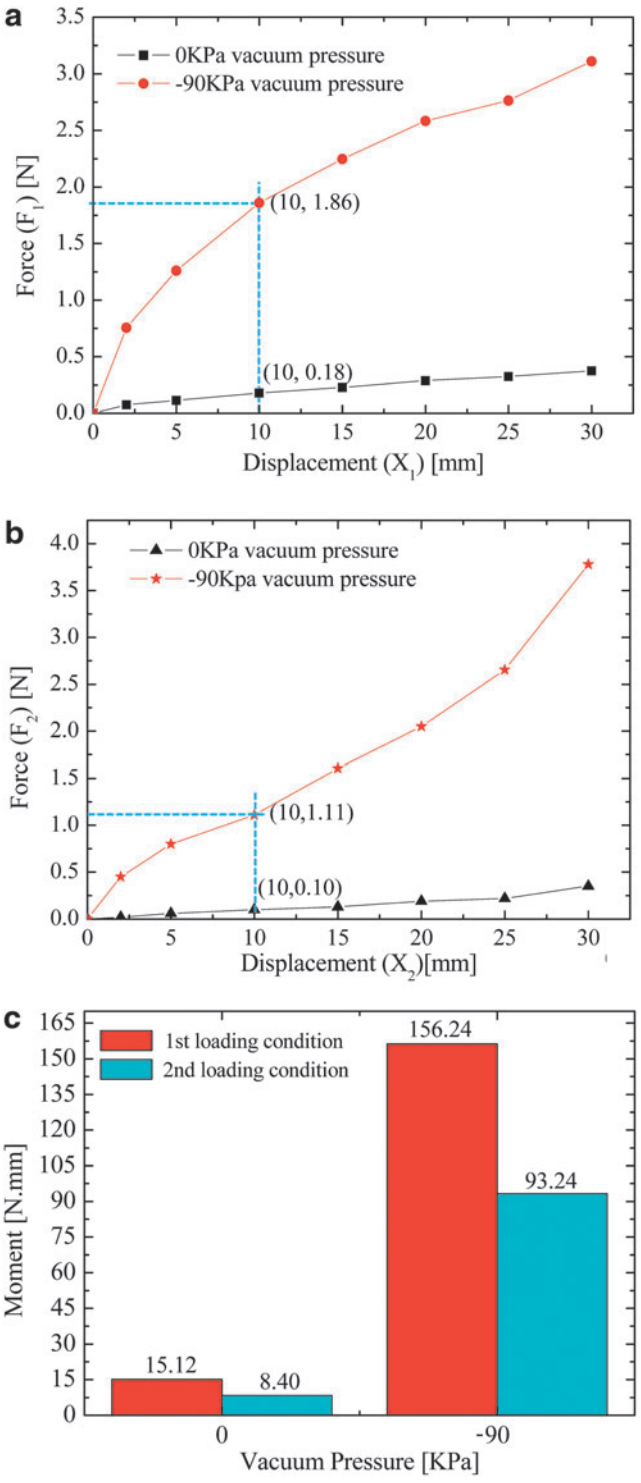

FIG. 7. Test results. **(a)** Force versus displacement in lateral bending plane. **(b)** Force versus displacement in transverse bending plane. **(c)** Maximum moment on two loading conditions with and without vacuum pressure. Color images available online at www.liebertpub.com/soro

the proposed robotic finger can change stiffness within a large range by controlling the vacuum pressure. For practical grasping, two working modes for the robotic gripper can be set: (1) contact mode when the vacuum pump is switched off, the soft hand performs passive adaption to objects at low stiffness and (2) force application mode when the vacuum pump is turned on. In the second mode, the soft hand stiffens to hold or manipulate or to resist external disturbances. In practical cases, the grasping is considered to be a failure when fingers show large displacement under external load because such displacement makes grasping unstable and less robust. It is essential to know the maximum value of external force that a finger can resist at the maximum allowable displacement. The maximum allowable displacement is set at 10 mm in this research, which is an empirical value. According to Figure 7a, the maximum force $F_{1max\text{-}90}$ is 1.86N (at vacuum pressure −90 KPa) and $F_{1max\text{-}0}$ is 0.18N (at vacuum pressure 0 KPa) at the allowable displacement $X_1 = 10$ mm. Obviously, on the axial bending plane (defined as the first loading condition), the finger can resist a much larger force of more than 10 times with vacuum pressure than that without vacuum pressure. Similarly, according to Figure 7b, the maximum force $F_{2max\text{-}90}$ is 1.11N (at vacuum pressure −90KPa) and $F_{2max\text{-}0}$ is 0.10N (at vacuum pressure 0 KPa) at allowable displacement $X_2 = 10$ mm. Again, the stiffness of the former is 10-fold more than the latter on the transverse bending plane (defined as the second loading condition). The maximum moments on the finger under the two loading conditions with different vacuum pressures can be calculated by Equation (8), where L is equal to 84 mm as shown in Figure 6a. The results are shown in Figure 7c, where the two red bars show the maximum moments under the first loading condition and the two blue bars show the maximum moments under the second loading condition.

$$M = FL \tag{8}$$

Figure 7c shows that whatever the loading condition is, finger stiffness increases by more than 10 times when particle jamming functions at −90 KPa vacuum pressure. In addition, under the same vacuum pressure, the maximum moment on the second loading condition is smaller than that of the first loading condition. It suggests that the better posture of manipulating or holding objects is to let the load direction be along the fingers' axial bending plane.

Compliance experiment

The compliance of muscle in human fingers forms a soft interaction with surroundings. This soft contact provides protection on other sensitive tissue and also facilitates fingers to adapt to objects with varied shapes and contours. It is a valuable inspiration for robotic grippers whose capability of compliance and adaption can promote reliability and robustness of grasping. As described in Section 2, most robotic grippers generally are designed for a specific set of objects with relatively regular shape or contour.

The comparison between the proposed gripper and a single soft actuator on object shape adaption is shown in Figure 8. Three white test models representing some common irregular features in our daily life are used. These features present a critical challenge for conventional, rigid robotic grippers and ordinary soft grippers. The integrated particle pack in the proposed design can effectively solve this problem. At natural state when the vacuum pressure is 0 KPa, the particles are loosely enclosed in the pack and the structure appears to be highly compliant and adaptive. This attribute leads to more

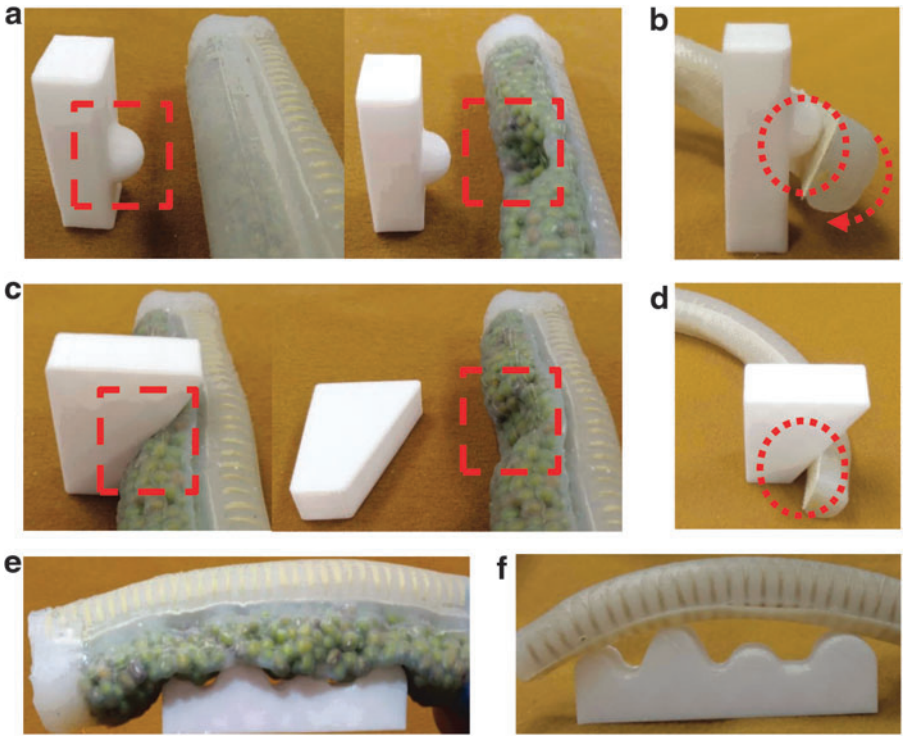

FIG. 8. Comparison between the proposed design and a single soft actuator in shape adaption: **(a)** conform to bump surface, **(b)** twist at bump surface, **(c)** conform to slant surface, **(d)** poor contact with slant surface, **(e)** confirm to uneven contour, and **(f)** poor contact at uneven contour. Color images available online at www.liebertpub.com/soro

sufficient contact with objects. When object manipulation is required, vacuum pressure is activated and the pack of particle is stiffened to provide a solid grip. For objects with a prominent bump surface, the proposed design can well adapt to the bump shape, as shown in Figure 8a. On the contrary, a large free space occurs between the object and the ordinary soft actuator, which may cause a negative twist on the actuator shown as the dashed line in Figure 8b. When the surface is slant, the proposed design shows good adaption as in Figure 8c, but the ordinary soft actuator cannot provide a stable envelope, as shown in Figure 8d. The difference in adaption performance becomes greater when the object shape is irregular with an uneven surface, as shown in Figure 8e, f. Therefore, our proposed design has fundamental advantages for stable and reliable grasping.

Grasping experiments

According to the experimental analysis above, our proposed robotic gripper has the merit of changeable stiffness in a large range. Besides, under room pressure, the fluid-like particles can function as a soft interface to provide better contact with objects through passive adaption. The grasping strategy is recommended as shown in Figure 9. The grasping process contains two steps: adaption (Fig. 9a) and stiffness enhancement (Fig. 9b). In the first step, the particle pack is soft and the whole finger presents high compliance, which allows sufficient contact between the finger and the object. When object manipulation is required, vacuum pressure is activated and the finger is stiffened by particle jamming to bear the load and resist external disturbance, as shown in Figure 9b.

Figure 10a–e shows some grasping snapshots. The bottle of water has a weight of 750 g, which is a heavy load for a soft robot. The first example shows a grasping attempt without particle jamming as shown in Figure 10a where the vacuum pressure is set to 0 KPa. Under this condition, the gripper manipulates the bottle flexibly and can move it in a short distance, but a large deformation twists the finger and the object suffers serious sliding, as shown in Figure 10b, and finally the grasp process fails, as shown in Figure 10c. On the contrary, after the fingers wrap around the bottle, the stiffness is strengthened under vacuum pressure −90 KPa, as shown in Figure 10d. The increased stiffness provided by particle jamming guarantees successful grasp even though the fingers still experience a small deformation. Besides, the grasping posture can be adjusted from Figure 10d, e for better object manipulation. Therefore, the easy and quick transition between low and high stiffness takes a further step toward the goal of imitating human grasp. Compared with the universal jamming gripper shown in Figure 2, our soft gripper can grasp objects in a variety of shapes without the limitation of

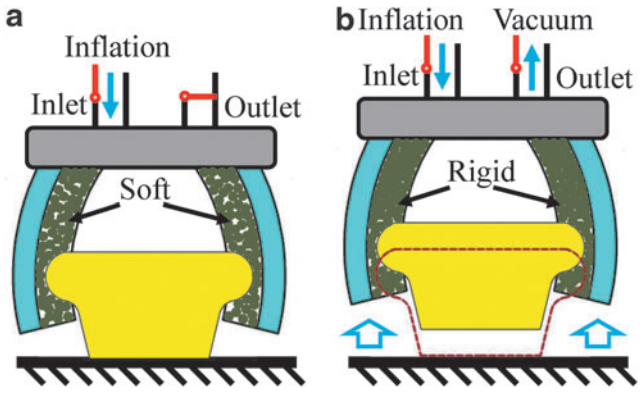

FIG. 9. Grasping strategy: **(a)** adaption with no vacuum, **(b)** stiffness enhancement with vacuum pressure on. Color images available online at www.liebertpub.com/soro

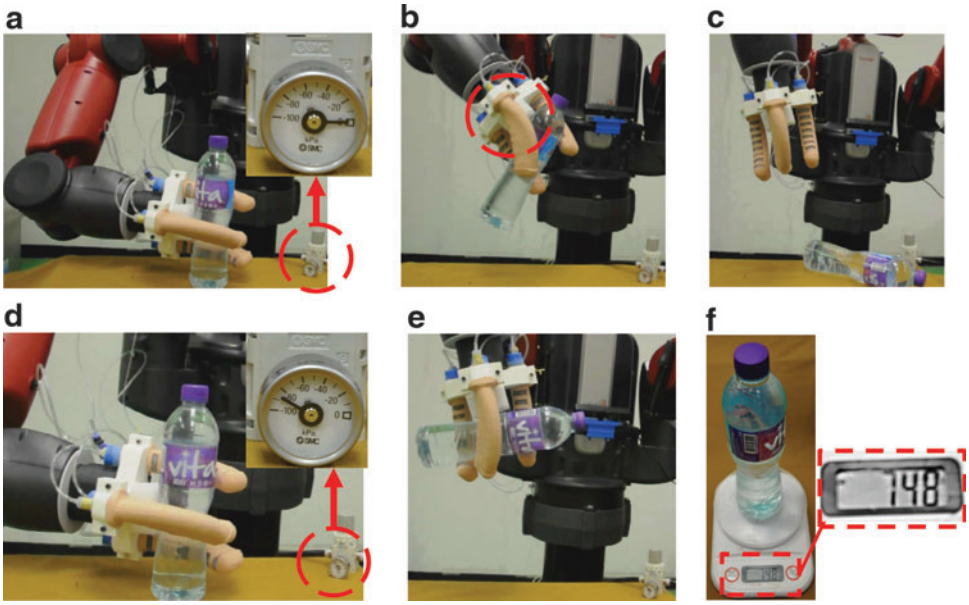

FIG. 10. Demonstration of grasping. **(a)** Grasping without vacuum pressure, **(b)** *large finger* deformation *under* heavy load, and **(c)** failed grasping with object falling down. **(d)** Grasping with vacuum pressure. **(e)** Successful grasping and reorienting to a better manipulating posture. **(f)** Object weight. Color images available online at www.liebertpub.com/soro

grasping postures. Meanwhile, stiffness variation allows the gripper to provide appropriate grasping force for different objects.

Conclusion

In this article, we have presented a soft robotic gripper with the capability of adaptive grasping and robust holding. The inherent merits result from the integrated design of fiber-reinforced soft bending actuator and particle jamming. The flexible but inextensible fibers arranged along the length of the soft actuator greatly simplify the manufacturing process, and the elastomeric elements augmented by fibers deform more equally with limited stress during pneumatic actuation, thus the actuator can withstand higher pressure and output larger forces. The particle-jamming method provides variable stiffness to the gripper by controlling vacuum pressure. The property of variable stiffness is attractive and is supported by experimental data and analysis. At low stiffness, the proposed gripper can perform dexterous grasping in natural state since it is highly flexible, compliant, and has passive adaption to object shape. When stiffened under vacuum pressure, the gripper gains extra stiffness from jammed particles and enables the gripper to keep firm holding of objects in spite of external force and other disturbances. The stiffness change within a large range allows the proposed hand to reproduce more functions and grasp capabilities of human hands. Besides, the manufacturing process of the soft gripper based on 3D printed molds and silicone rubber is quick and cost-effective. It is easy to be customized to build grippers with different sizes, shapes, and finger configurations. Considering all the advantages, our proposed robotic gripper has great potential for a wide range of applications in the service industry.

The proposed gripper based on the integration of two soft grasping principles provides a new way of thinking in soft robotics. The proposed design also has its own problems that may adversely affect its performance: (1) In natural state, the particles can be jammed passively when the finger is being bent due to reduction of particle chamber. Consequently, the bending range of a finger is affected. (2) The choice of an appropriate particle size is a challenge. A large size will greatly decrease the required particle quantity and weaken the compliance to object shape. Particles with a small size and irregular shapes such as coffee beans have poor fluidity, which also affects compliance. The determination of the optimal particle size, material, and shape is yet to be investigated. (3) The abrasion of membrane caused by friction with particles is inevitable. This will affect repeatability of the jamming effect. All these problems will be considered in our ongoing research through experimental and optimization methods.

Acknowledgment

This research is partly supported by an ITF grant from the Hong Kong Innovation and Technology Commission.

Author Disclosure Statement

No competing financial interests exist.

References

1. Bicchi A, Kumar V. Robotic grasping and contact: a review. International Conference on Robotics and Automation (ICRA), San Francisco, CA, 2000, pp. 348–353.
2. Okamura AM, Smaby N, Cutkosky MR. An overview of dexterous manipulation. International Conference on Robotics and Automation (ICRA), San Francisco, CA, 2000, pp. 255–262.
3. Lin H, Guo F, Wang F, Jia YB. Picking up a soft 3D object by ''feeling'' the grip. IJRR 2015;34:1361–1384.
4. Xydas N, Bhagavat M, Imin K. Study of soft-finger contact mechanics using finite elements analysis and experiments. International Conference on Robotics and Automation (ICRA), San Francisco, CA, 2000, pp. 2179–2184.
5. Kim S, Laschi C, Trimmer B. Soft robotics: a bioinspired evolution in robotics. Trends Biotechnol 2013;31:287–294.

6. Shepherd RF, Ilievski F, Choi W, Morin SA, Stokes AA, Mazzeo AD, *et al.* Multigait soft robot. Proc Natl Acad Sci 2011;108:20400–20403.
7. Wang Z, Chen MZQ, Yi J. Soft robotics for engineers. HKIE Trans 2015;22:88–97.
8. Ilievski F, Mazzeo AD, Shepherd RF, Chen X, Whitesides GM. Soft robotics for chemists. Angew Chem 2011;50: 1890–1895.
9. Polygerinos P, Zheng W, Overvelde JTB, Galloway KC, Wood RJ, Bertoldi K, *et al.* Modeling of soft fiber-reinforced bending actuators. IEEE Trans Robot 2015;31: 778–789.
10. Shepherd RF, Stokes AA, Freake J, Barber J, Snyder PW, Mazzeo AD, *et al.* Using explosions to power a soft robot. Angew Chem 2013;52:2892–2896.
11. Rateni G, Cianchetti M, Ciuti G, Menciassi A, Laschi C. Design and development of a soft robotic gripper for manipulation in minimally invasive surgery: a proof of concept. Meccanica 2015;50:2855–2863.
12. Renda F, Giorelli M, Calisti M, Cianchetti M, Laschi C. Dynamic model of a multibending soft robot arm driven by cables. IEEE Trans Robot 2014;30:1109–1122.
13. Huai-Ti L, Gary GL, Barry T. GoQBot: A caterpillar-inspired soft-bodied rolling robot. Bioinspir Biomim 2011;6:026007.
14. Laschi C, Cianchetti M, Mazzolai B, Margheri L, Follador M, Dario P. Soft robot arm inspired by the octopus. Adv Robotics 2012;26:709–727.
15. Anderson IA, Gisby TA, McKay TG, O'Brien BM, Calius EP. Multi-functional dielectric elastomer artificial muscles for soft and smart machines. J Appl Phys 2012;112:041101.
16. Pelrine R, Kornbluh R, Pei Q, Joseph J. High-speed electrically actuated elastomers with strain greater than 100%. Science 2000;287:836–839.
17. Shintake J, Rosset S, Schubert B, Floreano D, Shea H. Versatile soft grippers with intrinsic electroadhesion based on multifunctional polymer actuators. Adv Mater 2016;28: 231–238.
18. Takashima K, Sugitani K, Morimoto N, Sakaguchi S, Noritsugu T Mukai T. Pneumatic artificial rubber muscle using shape-memory polymer sheet with embedded electrical heating wire. Smart Mater Struct 2014;23:125005.
19. Niu X, Yang X, Brochu P, Stoyanov H, Yun S, Yu Z, *et al.* Bistable large-strain actuation of interpenetrating polymer networks. Adv Mater 2012;24:6513–6519.
20. Majidi C, Wood RJ. Tunable elastic stiffness with microconfined magnetorheological domains at low magnetic field. Appl Phys Lett 2010;97:164104.
21. Taniguchi H, Miyake M, Suzumori K. Development of new soft actuator using magnetic intelligent fluids for flexible walking robot. International Conference on Control Automation and Systems (ICCAS), Gyeonggi-do, Korea, 2010, pp. 1797–1801.
22. Amend JR Jr., Brown E, Rodenberg N, Jaeger H, Lipson H. A positive pressure universal gripper based on the jamming of granular material. IEEE Trans Robot 2012;28:341–350.
23. Cheng NG, Lobovsky MB, Keating SJ, Setapen AM, Gero KI, Hosoi AE, et al. Design and analysis of a robust, lowcost, highly articulated manipulator enabled by jamming of granular media. International Conference on Robotics and Automation (ICRA), Saint Paul, MN, 2012, pp. 4328–4333.
24. Cianchetti M, Ranzani T, Gerboni G, Nanayakkara T, Althoefer K, Dasgupta P, *et al.* Soft robotics technologies to address shortcomings in today's minimally invasive surgery: the STIFF-FLOP approach. Soft Robot 2014;1:122–131.
25. Wall V, Deimel R, Brock O. Selective stiffening of soft actuators based on jamming. International Conference on Robotics and Automation (ICRA), Seattle, WA, 2015, pp. 252–257.
26. Shintake J, Schubert B, Rosset S, Shea H, Floreano D. Variable stiffness actuator for soft robotics using dielectric elastomer and low-melting-point alloy. IEEE/RSJ International Conference on Intelligent Robots and Systems (IROS), Hamburg, Germany, 2015, pp. 1097–1102.
27. Brown E, Rodenberg N, Amend J, Mozeika A, Steltz E, Zakin M, *et al.* Universal robotic gripper based on the jamming of granular material. PNAS 2010;107:18809–18814.
28. Manti M, Hassan T, Passetti G, D'Elia N, Laschi C, Cianchetti M. A bioinspired soft robotic gripper for adaptable and effective grasping. Soft Robot 2015;2:107–116.
29. Pons JL, Ceres R, Pfeiffer F. Multifingered dextrous robotics hand design and control: a review. Robotica 1999; 17:661–674.
30. Deimel R, Brock O. A compliant hand based on a novel pneumatic actuator. International Conference on Robotics and Automation (ICRA), Karlsruhe, Germany, 2013, pp. 2047–2053.
31. Deimel R, Brock O. A novel type of compliant and underactuated robotic hand for dexterous grasping. IJRR 2016; 35:161–185.
32. Polygerinos P, Wang Z, Galloway KC, Wood RJ Walsh CJ. Soft robotic glove for combined assistance and at-home rehabilitation. Rob Auton Syst 2015;73:135–143.
33. Baumgart F. Stiffness—an unknown world of mechanical science? Injury 2000;31:14–84.

Address correspondence to:
Yonghua Chen
Department of Mechanical Engineering
The University of Hong Kong
Hong Kong 852
China

E-mail: yhchen@hku.hk